ISBN: 978-3-95450-179-3 doi:10.18429/JACoW-FEL2017-WEA01

EUROPEAN XFEL INJECTOR COMMISSIONING RESULTS*

B. Beutner†, DESY, Hamburg, Germany
on behalf of the European XFEL Accelerator Consortium and Commissioning Team

Abstract

In the first commissioning phase of the European XFEL SASE FEL driver linac, we demonstrated the design goals for the injector section. These goals include reliable operation of sub-systems and feasible beam parameters like emittance and bunch length of the beam produced by the RF gun. Of particular interest is the operation of long bunch trains with up to 2700 bunches with a 4.5 MHz repetition rate. In this presentation we will provide an overview of our experiences from the injector commissioning run including beam dynamics studies, diagnostics, and system performance.

INTRODUCTION

The European XFEL aims at delivering X-rays from 0.25 to up to 25 keV out of 3 SASE undulators lines [1, 2]. These undulators are driven by a superconducting linear accelerator based on TESLA technology [3]. European XFEL is build in an international collaboration of eleven countries.

In this paper we summarize results from the commissioning run of the injector in the first half of 2016, building on a previous report [4]. Results from the commissioning of the downstream part off the machine are summarised in [5].

The injector of the European XFEL consists of (compare Fig. 1) the RF gun, an booster and a linearliser accelerating module, a laser heater, and a diagnostic section. The main

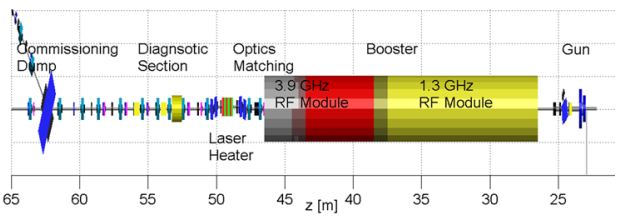

Figure 1: Injector of the European XFEL. Two RF stations (A1 at 1.3 GHz, and the AH1 at 3.9 GHz) are used for acceleration and longitudinal phase space shaping.

task of the injector is the production of low emittance beam at various charges ranging from 20 pC to 1 nC and the generation of a suitable longitudinal phase space correlation for downstream bunch compression. Nominal beam energy in the injector is 130 MeV.

As summarised in Table 1 we were able to demonstrate the design performance of the injector.

Time Structure

The unique feature of superconducting RF systems is the ability to generate long RF pulses and thus long bunch trains.

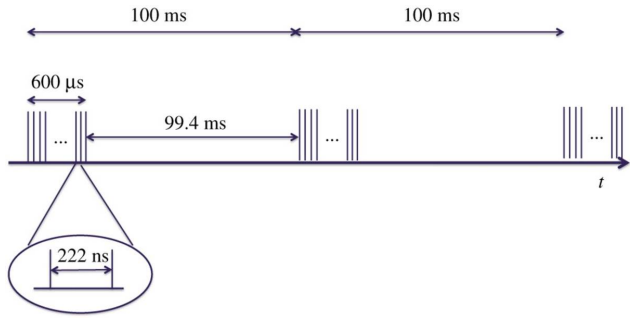

Figure 2: Time structure of the European XFEL bunch trains.

As visualised in Fig. 2 trains of up to 600 µs are generated with a 10 Hz repetition rate. With an intra train rate of up to 4.5 MHz the linac can deliver up to 2700 bunches per pulse. With a total of up to 473 kW beam power at full beam energy of 17.5 GeV. These bunches can be send to different undulator lines using fast kicker systems to allow flexible timing patterns for the user stations.

RF GUN

Gun Operation

During the injector run we restricted gun operation to limit the stress on the RF window. Either the gradient is driven to the maximum, for optimum emittance, or the pulse length is set to the design to demonstrate long train operation maintaining reasonable emittance. The parameters are shown in Table 2. These limitations are mainly imposed by the RF window. At PITZ[1] a setup with two RF windows is in operation allowing full design operation. For the time being we do not risk operation, however a later upgrade to a two-window setup is considered.

Fast Gun Start-up

Long RF pulses in the gun are challenging for gun operation. Up to 50 kW heat load are deposited in this normal conducting copper cavity from the RF. While the temperature stability requirements to keep the cavity on resonance is on the order of 0.05 deg C. Especially during startup the resonator is detuned since the RF load typically reacts much faster than the water regulation. The traditional solution to this problem is a slow increase of RF power. In such a operation, however, the startup takes about an hour with a risk of trips during the process. The process can be significantly accelerated by inducing an dynamic phase slope on the RF input signal. Such a slope is an effective frequency shift of the drive signal. A control system server is updating this phase slope according the determined detuning minimising the reflected RF power in the process [6]. With this

* Work supported by the respective funding agencies of the contributing institutes; for details please see http://www.xfel.eu
† bolko.beutner@desy.de

[1] Photo-injector test stand in DESY Zeuthen.

ISBN: 978-3-95450-179-3 doi:10.18429/JACoW-FEL2017-WEA01

Table 1: Injector Performance Defined in the Technical Design Report (TDR) Compared with Demonstrated Parameters during the Commissioning of the Injector

Quantity	TDR	achieved
Macro pulse repetition rate	10 Hz	10 Hz
RF pulse length (flat top)	650 µs	670 µs
Bunch repetition frequency within pulse	4.5 MHz	4.5 MHz
Bunch charge	20 pC–1 nC	20 pC–1 nC
Slice emittance (50 MV/m, 500 pC)	0.6 mm mrad	0.6 mm mrad

Table 2: Operation Modes of the RF Gun during the Injector Commissioning Run

	maximum pulse length	maximum gradient
foreward power	4.2 MW	6.61 MW
pulse length	650 µs	50 µs
gradient	50 MV/m	60 MV/m

procedure we can startup or recover gun operation in a few minutes instead of at least an hour significantly increasing machine availability.

PHASE SPACE STUDIES

Diagnostics Section

Phase space studies are done in a diagnostic section downstream of the laser heater. This section includes four-screen stations, a spectrometer arm, and a transverse deflecting RF structure (TDS) for longitudinal resolved studies. A unique feature of this diagnostics layout are fast kicker systems to kick individual bunches on off-axis screens [7]. In this configuration individual bunches out of the train can be analysed while the remaining bunches continue eventually to the SASE user stations. In Fig. 3 the operation of such semi-parasitic measurements is illustrated.

Projected Emittance

An important part of the injector commissioning was the demonstration of sufficient beam quality for the upcoming FEL commissioning. The focus these emittance optimisations was on the 500 pC operation mode. The other modes, namely th 50, 100, and 1000 pC options were studied with lower priority. The results of these optimisation runs are sumarised in Table 3.

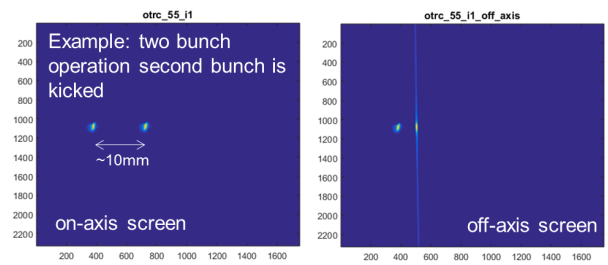

Figure 3: Semi-parasitic diagnostic operation. Two bunches are on the train. the second bunch is kicked using the kicker system. On the left hand side the full screen is inserted and both bunches are visible. Inserting the off-axis screen (right hand side) only the second bunch is visible while the first bunch continues through the beam dump.

The measured optimised emittance results are quite symmetric in the horizontal and vertical plane. This, however, is by choice. If we measure the emittance as function of the solenoid strength (an example is shown in Fig. 4) we observe an asymmetry between the planes. We choose the solenoid strength which minimises the geometric average $\sqrt{\varepsilon_x \cdot \varepsilon_y}$.

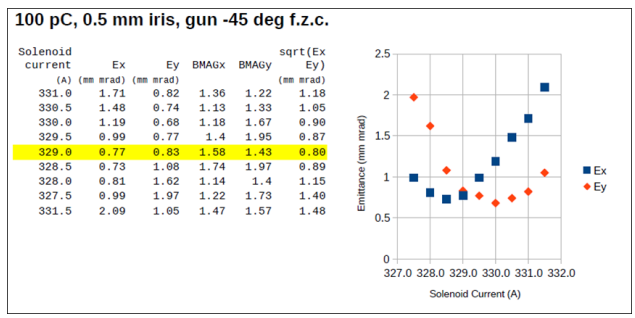

Figure 4: Summary of an emittance optimisation study. Normalised emittances in both planes are measured as a function of the solenoid current.

In 2017 corrector quads in the normal and skew direction are installed. Such correctors were studied at PITZ and are a promising tool to mitigate such asymmetries [8–10].

The discrepancies between the measured and simulated values in Table 3 have two main explanations. First of all most effort in terms of beam-time was put in the 500 pC mode, it is possible and to some extend expected, that modes with significantly different charge are not as well optimised.

Another reason for discrepancies, especially for lower bunch charges than 500 pC are issues with the screens for small beam spot sizes.

Transverse beam sizes are measured with scintillating screens (LYSO). Resolution of the screens is measured to be of the order of a few micron [11]. Typical transverse beam sizes to be resolved range from 40 to 100 µm, and are thus well above the resolution limit of the screens. Nevertheless, emittance measurements give unreasonable results at small beam sizes below about 50 µm, as they appear in four-screen sections. Only multi-quadrupole scans with enlarged beta-functions at the screen position give reliable results. This effect is under investigation.

ISBN: 978-3-95450-179-3 doi:10.18429/JACoW-FEL2017-WEA01

Table 3: Optimised Projected Normalised Emittances for the Different Bunch Charges Compared with Beam Dynamics Simulations. Uncertainties are the propagated statistical beam size measurement errors. Simulations are done with ASTRA [12].

charge	horizontal	vertical	simulation
50 pC	(0.56 ± 0.01) mm mrad	(0.64 ± 0.01) mm rad	0.27 mm rad
100 pC	(0.77 ± 0.02) mm mrad	(0.83 ± 0.03) mm rad	0.31 mm rad
500 pC	(1.28 ± 0.02) mm mrad	(1.23 ± 0.03) mm rad	1.15 mm rad
1 nC	(2.95 ± 0.02) mm mrad	(2.81 ± 0.03) mm rad	1.83 mm rad

Slice Emittance

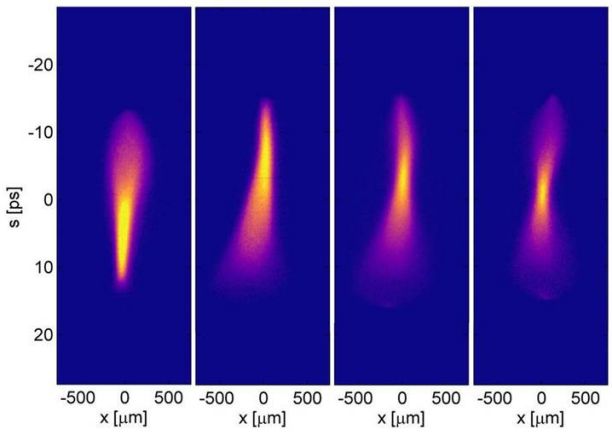

Figure 5: An example of a slice emittance measurement using the four-screen setup, as described for the projected measurements, in combination with a transverse deflecting structure.

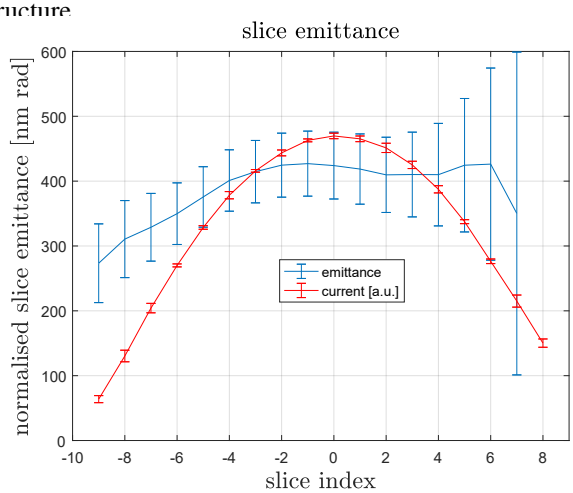

Figure 6: An example slice emittance measurement. 200 pC beam accelerated with 60 MV/m in the gun. The current profile as well as the slice emittance is plotted.

In the described diagnostics layout a TDS is used for longitudinal resolved measurements (see Figures 5, 6, 7). This allows for studies of the emittance of individual slices. Such slices are still much longer than the corporation length but still a very good approximation to this relevant number for the FEL gain. In contrast to the projected emittance results shown earlier here the agreement with the expected results from calculations is much better. This is another indication for issues with the diagnostics of small beam spots.

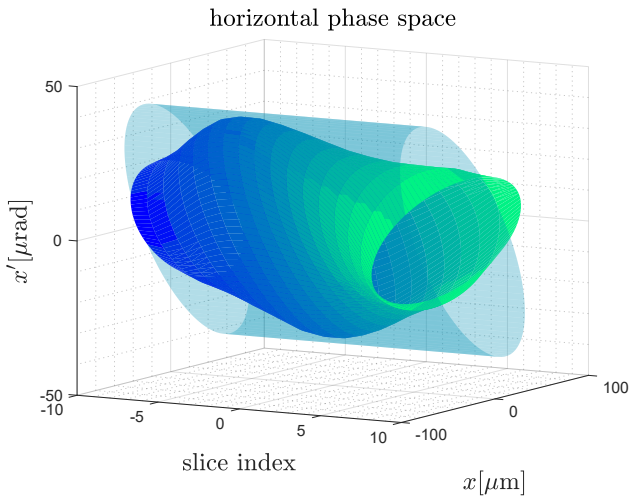

Figure 7: A representation of the Twiss phase space ellipses of the data shown in Fig. 6. The design optics is indicated by the transparent "tube".

Using not only the spot size to fit the phase-space beam moments but include the slice centroid positions as well we can determine the centroid position of each slice in phase-space. This allows us to recover the projected emittance from the slice measurements (see Fig. 8). This values have some uncertainty, since non-uniformities in the kicker fields

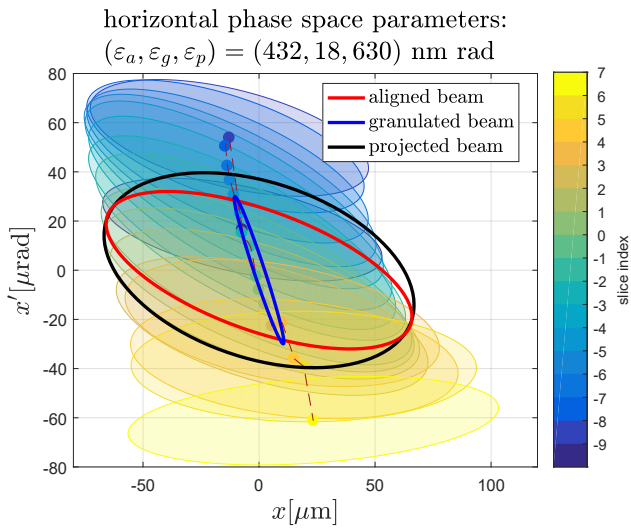

Figure 8: From the data in Fig. 6 we reconstructed the projected beam parameters. The relative "rotation" as well as centroid shifts in phase space needs to be taken into account [13, 14].

ISBN: 978-3-95450-179-3 doi:10.18429/JACoW-FEL2017-WEA01

were only partially included, but still the agreement with the expected projected emittance is good.

The measurements discussed so far utilised the fast-kicker system diagnostic section in semi-parasitic operation. This measurements are fast and very well suited for scans of parameter spaces for machine optimisation. However, better results can be achieved by multi-quadrupole scans on a single screen. In such scans the beam spot size is chosen much larger than in the FODO configuration avoiding resolution issues and the longitudinal resolution of the TDS setup can be optimised. In addition more than four data points are available increasing the accuracy of the beam moment fit. With measurements using this technique we achieved normalised emittances down to 0.4 mm mrad slice emittance for 500 pC for moderate gun gradients (compare Fig. 9).

Phase Space Tomography

More detailed phase-space beam dynamics studies are possible by using not only the beam spot-sizes but the profile information from a modified multi-quad scan [15]. With tomographic methods the phase-space density distribution can be recovered (compare Fig. 10). While the phase-space dynamics in the injector are relatively straightforeward we

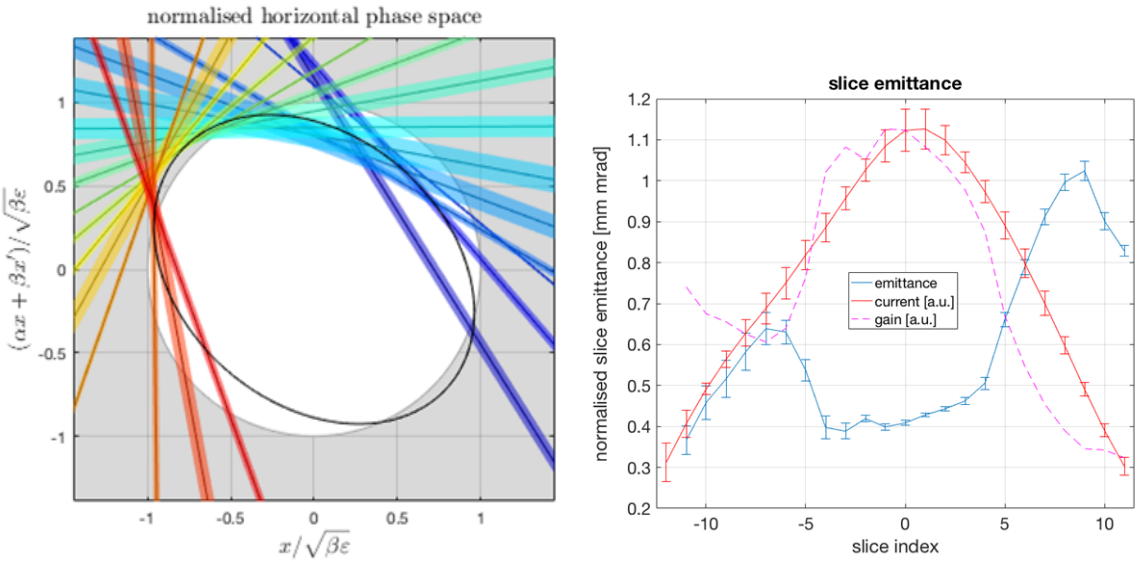

Figure 9: An example of an optmised 500 pC beam at 53 MV/m gun gradient using a multi-quad scan. The phase space fit indicated on the left hand side corresponds to the core slice of the bunch.

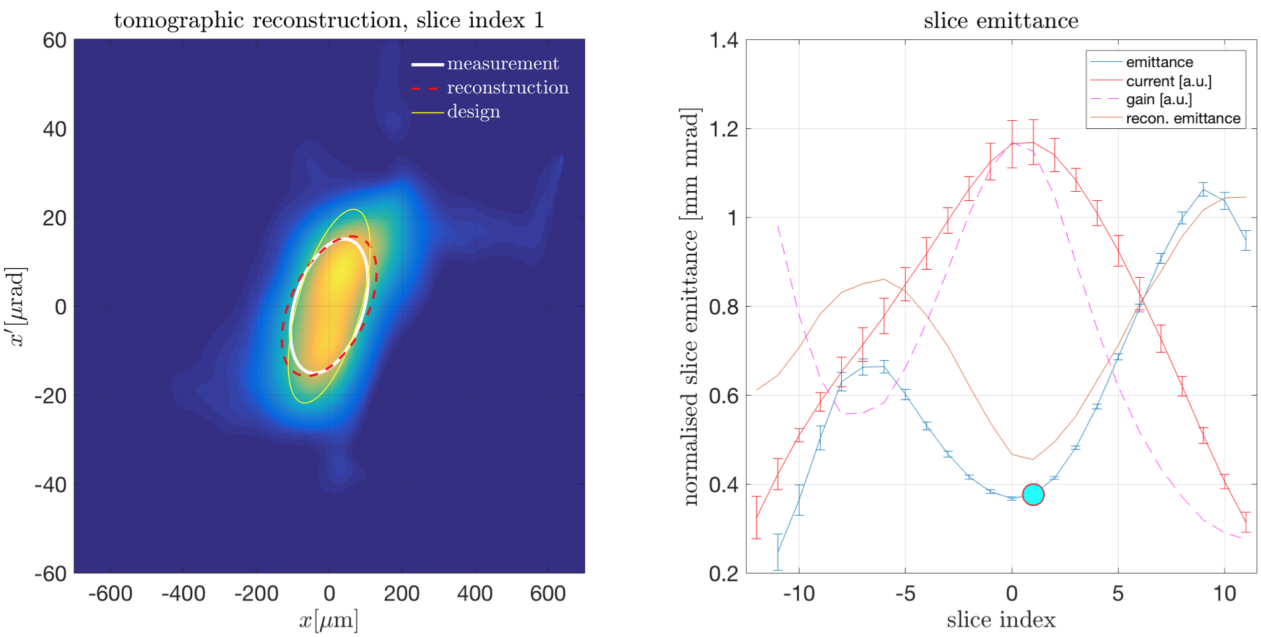

Figure 10: Tomographic reconstruction of the core slice from a slice emittance measurement. The phase space density distribution is shown in the left hand plot together with the design and reconstructed Twiss ellipses. On the right hand side the corresponding emittances are shown along the bunch.

ISBN: 978-3-95450-179-3 doi:10.18429/JACoW-FEL2017-WEA01

expect more interesting studies with this techniques in the bunch compressor sections downstream of the injector.

SUMMARY AND OUTLOOK

In summary we report that the injector of the European XFEL was commissioned to design performance. However optimisations are still possible. Especially the operation at full gun gradient with long bunch trains needs to be established for long-train user operation foreseen for 2018. On the beam dynamics and diagnostic side issues with the emittance measurements, namely the overestimation of small beam sizes is under investigation and will be worked on in the future.

Another topic which was not covered in this discussion is the laser heater system. Even though we have first demonstrations of its utility (see [16]) systematic studies during FEL beam delivery are foreseen in the future.

ACKNOWLEDGEMENTS

The fabrication, testing and installation of the injector components were only possible with a tremendous effort from all partners - and still it is needed from the operators and scientists doing the commissioning. The author likes to thank the complete team for their work and support.

REFERENCES

[1] M. Altarelli *et al.* Ed., "The European X-Ray FreeElectron Laser - Technical Design Report", DESY, Hamburg, Germany, Rep. DESY 2006-097, July 2007.

[2] R. Brinkmann *et al.* Ed., "TESLA XFEL Technical Design Report Supplement", DESY, Hamburg, Germany, Rep. DESY 2002-167, March 2002.

[3] R. Brinkmann *et al.* Ed., "TESLA Technical Design Report - Part II: The Accelerator", DESY, Hamburg, Germany, Rep. DESY 2001-011, March 2001.

[4] F. Brinker, "Commissioning of the European XFEL Injector", in *Proc. IPAC2016*, Busan, Korea, 2016, https://doi.org/10.18429/JACoW-IPAC2016-TUOCA03

[5] W. Decking and H. Weise, "Commissioning of the European XFEL Accelerator", in *Proc. IPAC2017*, Copenhagen, Denmark, 2017, https://doi.org/10.18429/JACoW-IPAC2017-MOXAA1

[6] Y. Renier *et al.*, "Fast Automatic Ramping of High Average Power Guns", in *Proc. IPAC2017*, Copenhagen, Denmark, 2017, https://doi.org/10.18429/JACoW-IPAC2017-TUPIK052

[7] C. Wiebers *et al.*, "Scintillating Screen Monitors for Transverse Electron Beam Profile Diagnostics at the European XFEL", in *Proc. IBIC2013*, Oxford, UK, paper WEPF03, 2013.

[8] M. Scholz and B. Beutner, "Studies of the Transverse Beam Coupling in the European XFEL Injector", presented at FEL 2017, Santa Fe, NM, USA, paper TUP005, 2017.

[9] M. Krasilnikov *et al.*, "Electron Beam Asymmetry Compensation with Gun Quadrupoles at PITZ", presented at FEL2017, Santa Fe, NM, USA, paper WEP007, 2017.

[10] Q. Zhao, M. Krasilnikov *et al.*, "Beam Asymmetry Studies with Quadrupole Field Errors in the PITZ Gun Section", presented at FEL2017, Santa Fe, NM, USA, paper WEP010, 2017.

[11] G. Kube *et al.*, "Transverse Beam Profile Imaging of few-Micrometer Beam Sizes Based on A Scintillator Screen", in *Proc. IBIC2015*, Melbourne, Australia, 2015, https://doi.org/10.18429/JACoW-IBIC2015-TUPB012

[12] Y. Kot, private comunication.

[13] C. Mitchell, "A General Slice Moment Decomposition of RMS Beam Emittance", arXiv:1509.04765v1[physics.acc-ph], 2015.

[14] V. Balandin, private comunication.

[15] M. Scholz and B. Beutner, "Electron Beam Phase Space Tomography at the European XFEL Injector", in *Proc. IPAC2017*, Copenhagen, Denmark, May 2017, https://doi.org/10.18429/JACoW-IPAC2017-WEPAB024

[16] M. Hamberg *et al.*, "Electron Beam Heating with the European XFEL Laser Heater", presented at FEL2017, Santa Fe, NM, USA, paper WEP018, 2017.